ACS OMEGA

http://pubs.acs.org/journal/acsodf

Article

Optimized Preparation of a Low-Working-Temperature Gallium Metal-Based Microencapsulated Phase Change Material

Kaixin Dong, Takahiro Kawaguchi, Yuto Shimizu, Hiroki Sakai, and Takahiro Nomura*

Cite This: *ACS Omega* 2022, 7, 28313−28323

Read Online

ACCESS | Metrics & More | Article Recommendations | Supporting Information

ABSTRACT: Gallium has been considered for application in the thermal management of electronic equipment because of its high heat transfer ability and heat storage density. To address the issues of metal corrosion and leakage, a microencapsulation method, through which a stable corrosion-resistant ceramic shell can be formed from the liquid metal, is proposed. In this study, an optimized fabrication method for a microencapsulated phase change material (MEPCM) consisting of liquid-state Ga droplets, possessing high durability and heat storage density, is presented. A fabrication route comprising particle formation, hydrothermal treatment, and calcination is proposed. In particular, the thickness and crystal size of the GaOOH shell are controlled by changing the pH during hydrothermal treatment to produce a highly durable shell. The morphology and microstructure, phase composition, heat storage capacity, and durability of the prepared Ga-MEPCM are investigated. In addition, treatment conditions and the shell formation mechanism are analyzed. The results show that pH 9 is the most suitable shell-forming condition, at which the thickest Ga_2O_3 shell with the smallest crystal size can be produced, which is beneficial for ensuring durability. The MEPCM achieved 200 cycles without leakage and 300 cycles without shape deformation with a high heat storage density of 369.4 J·cm^{-3}.

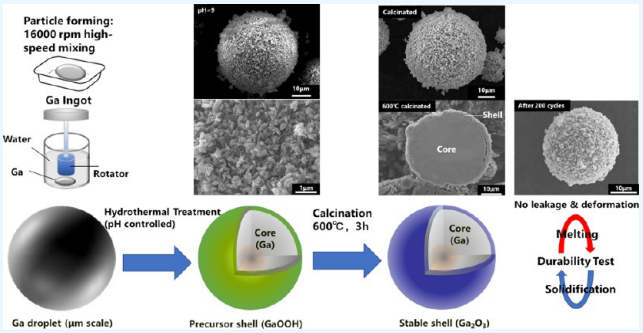

1. INTRODUCTION

In recent decades, the rapid development of information technology (IT) has significantly changed the world with respect to both industry and people's daily lives. Integrated circuits (ICs) play an important role in devices, such as personal computers (PCs) and smartphones. During the operation of ICs, electricity is consumed and heat is generated; however, ICs have a safe running temperature range for which higher temperatures may affect the service life of the circuit, e.g., the safe temperature range of a CPU is below 85 °C and that of a diode laser chip is below 65 °C. The trend of electronic equipment is toward miniaturization and high integration, especially with the rapid development of artificial intelligence (AI), 5G communication, and the aerospace industry. More powerful and smarter devices require a higher density of ICs to manage a large number of high-speed calculations, which will significantly increase the heat generated in the device. Therefore, the thermal management of electronic equipment is required to maintain the temperature of the device in the range of safe running.[1−3]

Thermal energy storage based on phase change materials (PCMs) is a promising technology for passive thermal management that does not require additional energy consumption. PCMs can absorb large amounts of heat during their phase transition (usually melting), which can contribute to the temperature control of a device. PCMs with low melting temperatures (<100 °C) have shown potential for application in thermal management systems of EV batteries and electronic devices because they can be cyclically used without any additional energy input; they can also be used to support existing active thermal management systems. Safdari et al.[4] performed a numerical investigation of encapsulated PCM and air cooling-based passive−active battery thermal management system, the results showed that PCM could greatly decrease the speed temperature increase of the battery for a long time when the temperature reaches the melting temperature of PCM. Kandasamy et al.[5] used a novel PCM package for thermal management of portable electronic devices and investigated the performance, the experimental and numerical results both proved the function of PCM in decreasing the speed of temperature increase and they gave many contributing conclusions for the design of the PCM-based thermal management system. Tomizawa et al.[6] investigated the PCM-based thermal management system of smartphones numerically and experimentally. They used resin microencapsulated paraffin wax as MEPCM to conduct the experiment, when a

Received: May 5, 2022
Accepted: June 22, 2022
Published: August 8, 2022

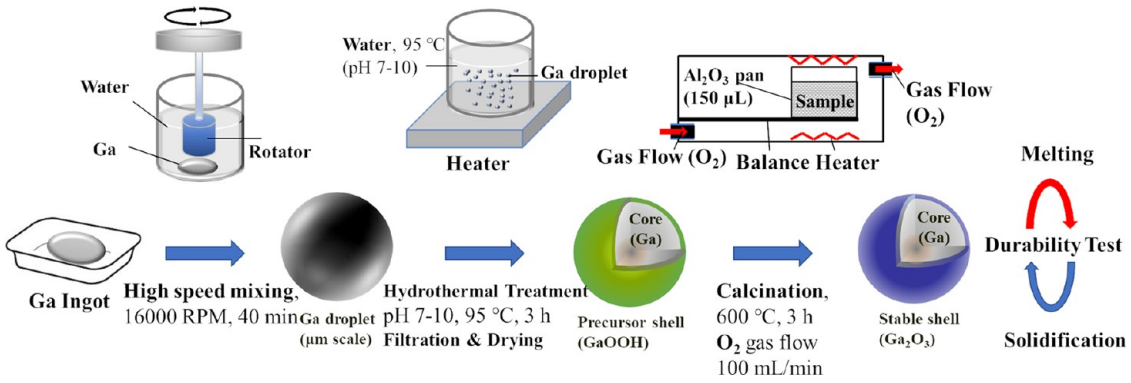

Figure 1. Schematic diagram of the $Ga@Ga_2O_3$ MEPCM fabrication process.

PCM sheet is used, the maximum temperature of the system is decreased and the time to reach the maximum temperature is greatly delayed, proving the function of PCM in smartphone thermal management. Ling et al.[7] reviewed the thermal management systems for electronic components and batteries and photovoltaic modules using PCM-based latent heat storage technology widely. They introduced the excellent function of PCM to be used in temperature moderation and many successful practical applications or research. PCMs can be divided into three types according to their composition: organic (acids, sugar alcohols), inorganic (hydrated salts), and metal PCMs. However, organic and inorganic PCMs have limitations, as their low thermal conductivity will lead to an unacceptable low heat transfer rate, which renders their use in practical thermal management difficult. Even though there have been many studies[8−10] regarding the enhancement of thermal conductivity by fabricating composites, the results demonstrate low values (lower than 30 $W{\cdot}m^{-1}{\cdot}K^{-1}$), and the density of these PCMs is low, which makes achieving a high heat storage density in a suitable volume for device miniaturization challenging.

Because of the limitations associated with conventional organic and inorganic PCMs regarding thermal management, we suggest gallium metal as a novel low-working-temperature PCM. Low-melting-temperature metal gallium has a much higher thermal conductivity (40 $W{\cdot}m^{-1}{\cdot}K^{-1}$) than any other organic/inorganic PCM, and the density of Ga (6.086 $g{\cdot}cm^{-3}$ at melting temperature) is very high, which can easily lead to a high heat storage density in a small volume. Ge et al.[11] reviewed the potential of low-melting-point metals as a new class of phase change materials, and pointed out the possibility of Ga or Ga-based alloys to be used as PCM in 2013. They also mentioned that corrosion of liquid metal is a very big challenge for practical applications. Ga has also been proved to have many advantages in the thermal management of spacecraft electronic equipment. Peng et al.[12] investigated the melting behavior and heat transfer performance of Ga under normal and microgravity conditions, and their results showed that Ga can reduce the melting time by over 96.4% compared with conventional materials like n-octadecane and increase the total energy storage capacity by 123.3% under microgravity, which demonstrates the potential of Ga to be used as a spacecraft thermal management material.

The issue of the practical utilization of PCM is the corrosion and electricity leakage of liquid-state metal. To address this limitation, the microencapsulation of PCMs has been considered by many researchers, e.g., fabricating core−shell structure microencapsulated PCM to maintain the melted PCM in the shell during the heat storage process, some previous studies have successfully fabricated organic or polymer shells for many PCMs.[13−15] However, the durability and corrosion resistance of these encapsulated PCMs were not proved or proved to be poor. With a highly durable and corrosion-resistant shell, metal PCMs could be used in electrical devices, despite the risks of corrosion and leakage. To solve the corrosion problem of metals and increase their durability, ceramic shells such as metal oxides were developed. In previous studies, Al and Al alloy-based microcapsules have been developed using a water treatment-calcination method. In 2016, Nomura et al. successfully fabricated an $Al\text{-}Si@Al_2O_3$ MEPCM by hydrothermal treatment and calcination and described the shell formation mechanism and process.[16] With a further modification of the preparation method involving the addition of $Al(OH)_3$, Sheng et al.[17,18] achieved a highly durable MEPCM via Boehmite treatment and high-temperature calcination, in which the MEPCM endured 3000 thermal cycles without core leakage or damage. Zou et al.[19] developed a Sn-based MEPCM using a double coating method, in which a PMMA (polymethyl methacrylate) layer was first fabricated via ultrasonication, and a SiO_2 shell was then produced using a sol−gel method; finally, the PMMA shell was decomposed to form an $Sn@SiO_2$ MEPCM with voids to resist expansion. Our group has also studied the possibility of forming Ga microcapsules, in which a Ga-MEPCM treated in boiled water was fabricated, and the best calcination temperature for forming a microcapsule was investigated; however, the MEPCM showed very poor durability of less than 10 cycles.[20] The fabrication mechanism and optimum fabrication conditions remain unclear, and a fabrication method for practical low-melting-temperature metal MEPCMs is yet to be established.

In this study, the optimized hydrothermal treatment and heat treatment of Ga metal were conducted to produce a highly durable and stable Ga-MEPCM. We chose Ga_2O_3 as the shell of the MEPCM, because of its corrosion resistance, good mechanical properties, and chemical stability, also, Ga_2O_3 can be easily produced by the oxidization of Ga metal by the hydrothermal-calcination method. The particle size and pH during water treatment were adjusted, and the shell structure and shell thickness were carefully examined. Additionally, the durability and heat storage capacity of the MEPCM were investigated. The shell formation mechanism was further examined, and the durability of the MEPCM was found to be significantly enhanced. The target of this research is to produce

https://doi.org/10.1021/acsomega.2c02801
ACS Omega 2022, 7, 28313−28323

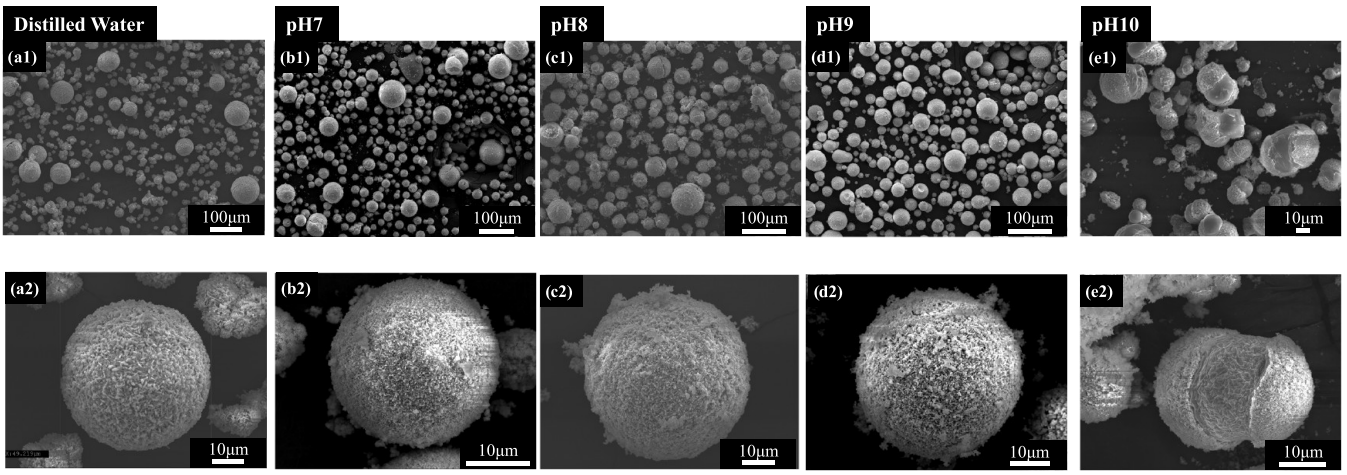

Figure 2. Surface SEM images of chemical-treated Ga@GaOOH microcapsules in (a1, a2) distilled water and (b1, b2), pH 7, (c1, c2) pH 8, (d1, d2) pH 9, and (e1, e2) pH 10 solutions at 95 °C for 3 h.

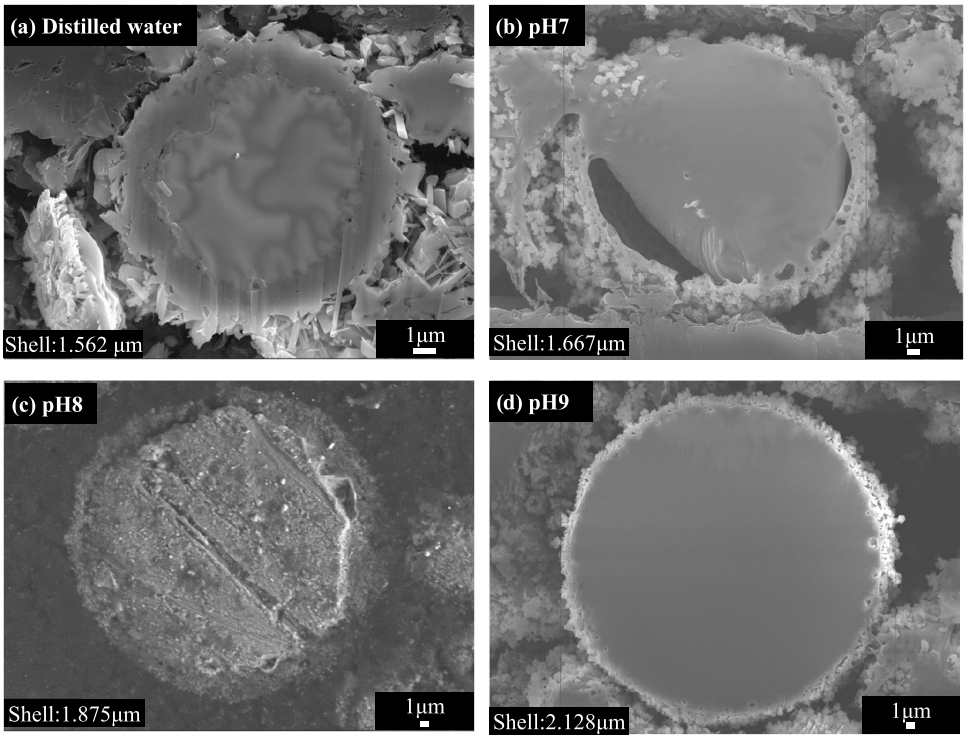

Figure 3. Cross-section SEM image and shell thickness of Ga@GaOOH MEPCM fabricated in (a) distilled water and (b) pH 7, (c) pH 8, and (d) pH 9 solutions.

a long durable, high heat storage density MEPCM, which is expected to be used in the field of low-temperature heat storage and thermal management, such as passive thermal management of spacecraft, electronic parts, laptops, and smartphones, or in thermal interface materials to form a high thermal conductive composite with heat storage ability.

2. EXPERIMENTAL SECTION

2.1. Preparation of MEPCM. A Ga ingot (purity 99.99%, Kojundo Chemical Laboratory Co. Ltd., Japan) was used as a PCM. It has a melting point of 29.8 °C and latent heat of 80.1 $J{\cdot}g^{-1}$; with the high density of Ga, the volume heat storage density can reach 488.2 $J{\cdot}cm^{-3}$. Figure 1 shows a schematic of the Ga-MEPCM fabrication process. In the first step, the Ga ingot was mixed in a high-speed mixer at 16 000 rpm for 40 min at 40 °C to form Ga droplets; the droplet formation time was adjusted to 40 min to yield the MEPCM with smaller particle sizes, with the aim of reducing the amount of expansion during thermal cycles. High-speed mixing is a common method for forming liquid droplets at the micrometer scale, and it uses the shearing force of the matrix liquid to form the liquid metal into small spherical droplets.[21] Second, Ga droplets were added to 100 mL of distilled water (pH around 6) in a poly(tetrafluoroethylene) (PTFE) container heated to 95 °C (a PTFE container was used instead of a glass beaker to prevent the wetting effect of Ga, and also decrease the reaction temperature to reduce the number of fragments generated through water boiling). An NH_3 solution was added to achieve various pH values (7−10), and the sample was treated for 3 h;

https://doi.org/10.1021/acsomega.2c02801
ACS Omega 2022, 7, 28313−28323

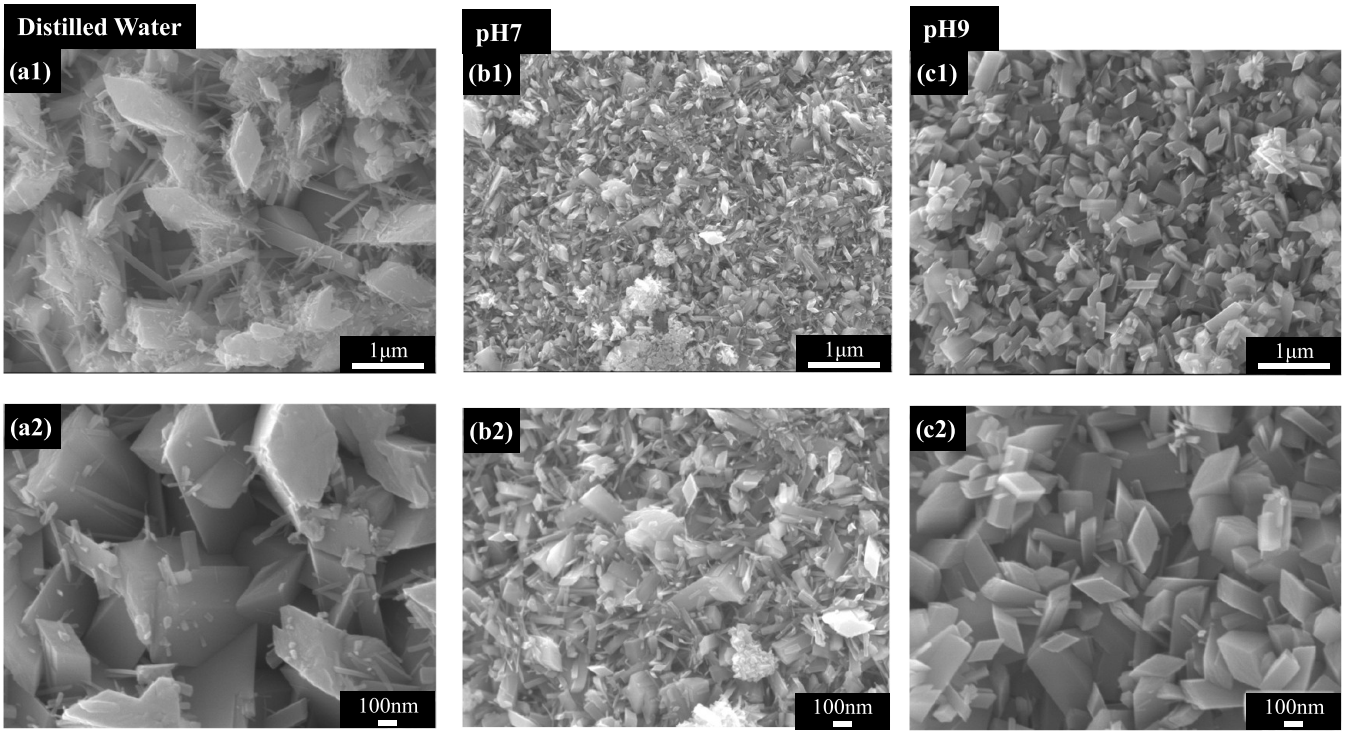

Figure 4. High-magnification surface SEM images of Ga@GaOOH MEPCM fabricated in (a1, a2) distilled water and (b1, b2) pH 7 and (c1, c2) pH 9 solutions under the same magnification.

each pH value was maintained for 15 min during the treatment. Distilled water treatment without the addition of ammonia solution was also performed as a reference. After the hydrothermal treatment, the Ga@GaOOH MEPCM sample was filtered and dried for 1 day at 40 °C. Finally, the Ga@GaOOH MEPCM was calcined at 600 °C for 3 h under an oxygen gas flow (100 mL/min) to form a stable Ga@Ga_2O_3 MEPCM using a Mettler Toledo TG/DSC 3+ thermogravimetry device.

2.2. Characterization. The surface and cross-section morphology of the Ga microcapsules at each stage were observed using scanning electron microscopy (SEM; JEOL, JSM-7001FA), and energy-dispersive X-ray spectroscopy (EDS) analysis was performed to investigate the elemental distribution of the cross-section. The cross-section of the microcapsule was prepared using a cross-section polisher (CP, JEOL cross-section polisher). The chemical and phase compositions of the MEPCM were determined via X-ray diffraction (XRD, Rigaku Miniflex600, D/teX Ultra2, Cu Kα). The weight change and temperature response during calcination were characterized using a Mettler Toledo TG/DSC 3+ thermogravimetry (TG) device. The heat storage capacity and phase change characteristics of the MEPCM were measured using a differential scanning calorimetry (DSC) analyzer (DSC-823e, Mettler Toledo) under an Ar atmosphere at a heating and cooling rate of 1 K·min^{-1}. The durability testing of the MEPCM was also performed via DSC, wherein Ga-MEPCM samples were cyclically heated and cooled from 50 to −50 °C to simulate practical melting−solidification thermal cycles. After durability testing, the sample was also measured via DSC and SEM/EDS to investigate its performance.

3. RESULTS AND DISCUSSION

3.1. Morphology and Microstructure of MEPCM Samples. Figure 2 shows the surface and cross-section images of Ga@GaOOH MEPCMs obtained after water/hydrothermal treatment. Every sample possessed a complete shell, except that treated at pH 10. At pH 10, although an oxidized shell of Ga was generated, the shell did not have sufficient strength and thickness to maintain its shape, and the microcapsules collapsed after drying. The MEPCMs treated in water and pH 7−9 solutions were nonuniformly covered by precipitated crystals of oxidized Ga. Among the pH-adjusted samples, the sample treated at pH 9 showed the best surface conditions, with a low breaking ratio and fewer cracks. We also measured the particle size distribution of the successfully fabricated MEPCMs using a HORIBA particle size analyzer LA950, the results are shown in Figure S1, all of the samples showed a particle size ranging from 20 to 50 μm. To determine the most suitable treatment conditions for high-durability MEPCMs, we examined the cross-section of each sample to check the shell thickness; the results are shown in Figure 3. The SEM-estimated shell thicknesses of the samples treated in water and solutions with pH values of 7, 8, and 9 were 1.562, 1.667, 1.875, and 2.128 μm, respectively. This result indicates that the shell thickness of the MEPCMs increased with increasing pH (in the range of 7−9). Notably, the crystal size of each MEPCM sample was different.

Figure 4 shows high-magnification SEM images of the MEPCMs treated in distilled water and pH 7 and pH 9 solutions, where the crystal size obtained in the high-pH sample is much smaller than that in water and the pH is unadjusted (close to 6). As estimated via SEM, the crystal size obtained at pH 9 is only 30% of that obtained in water. Krehula et al.[22] and Qian et al.[23] also reported the influence of pH and ammonia solution on the crystal size during the

https://doi.org/10.1021/acsomega.2c02801
ACS Omega 2022, 7, 28313−28323

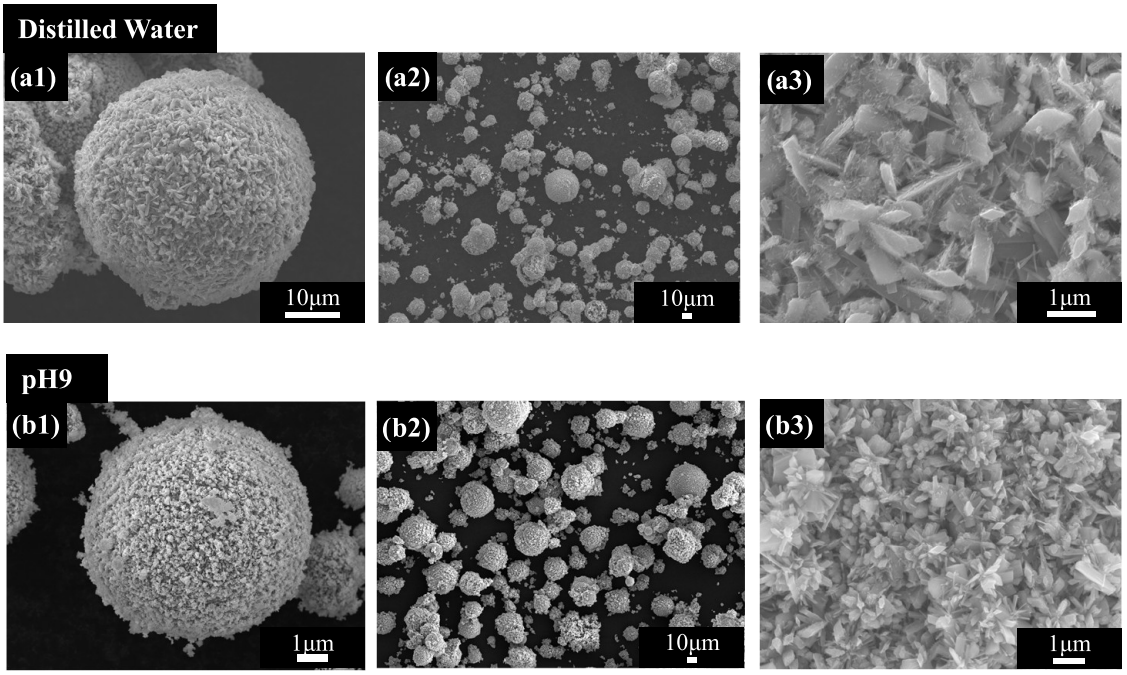

Figure 5. Surface SEM images of O_2 gas-calcined Ga@Ga_2O_3 microcapsules (a1, a2, a3) in distilled water and (b1, b2, b3) pH 9 solution at 600 °C, maintained for 3 h.

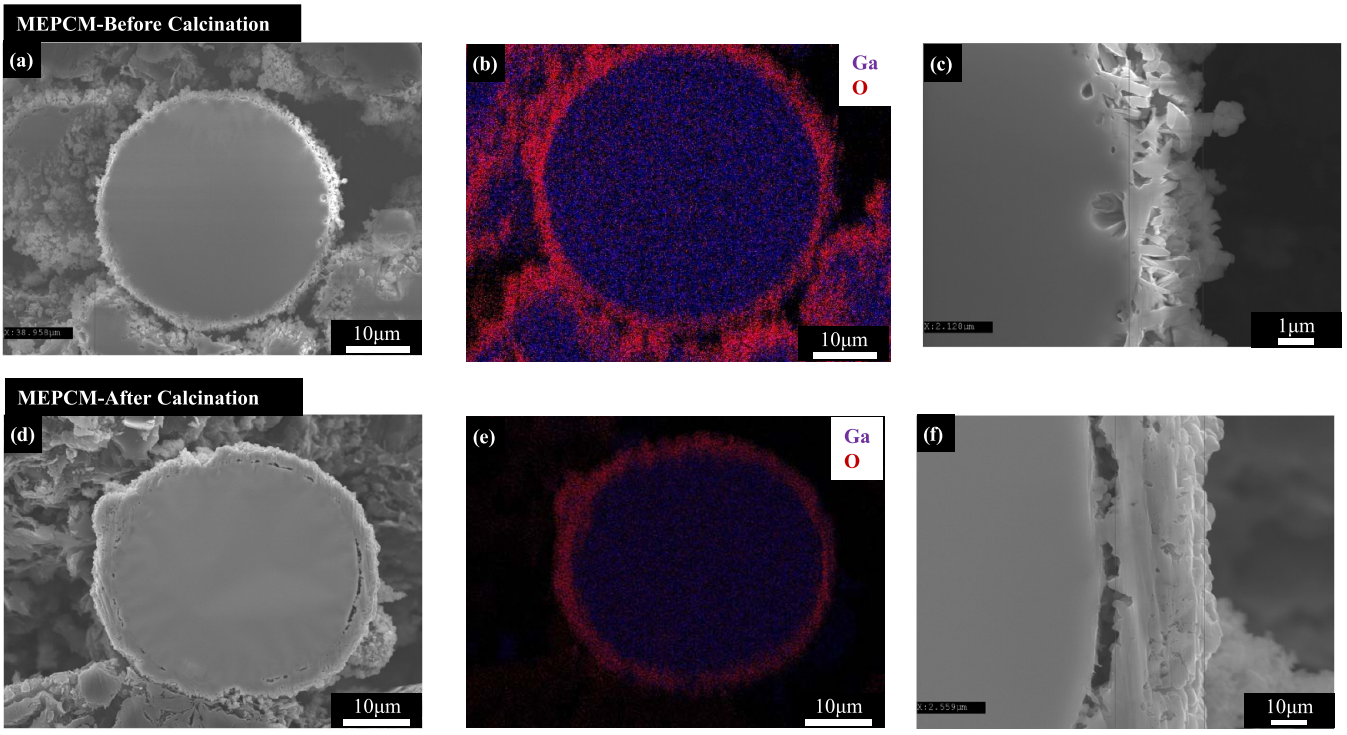

Figure 6. Cross-section SEM images (a, c, d, f) and EDS mapping (b, e) of pH 9-treated MEPCM before and after calcination.

generation of GaOOH, where the size of the generated GaOOH crystals decreased with increasing pH value in a given range. Zhao et al.[24] investigated the size and morphology of GaOOH. We think the biggest considerable mechanism for the crystal size change is because high pH results in a high OH^- concentration that can accelerate the generation of GaOOH crystals (reactions 1 and 2 in Section 3.2), with the generation of more crystals, the size of each crystal will be smaller. Different from the previous studies of free growth, in our study, the surface area of the shell, treatment time, and temperature were determined, and the space for the crystals to grow is the same. As for the function of NH_4^+, Qian et al. also reported a phenomenon where ammonia water could coordinate with Ga^{3+} to produce $Ga(NH_3)_x^{3+}$ complexes, which can also accelerate the nucleation and growth of $Ga(OH)_4^-$. A smaller crystal size could provide higher mechanical strength for the shell to resist deformation during thermal cycles, and with a smaller crystal size, the number and size of structural voids will

https://doi.org/10.1021/acsomega.2c02801
ACS Omega 2022, 7, 28313−28323

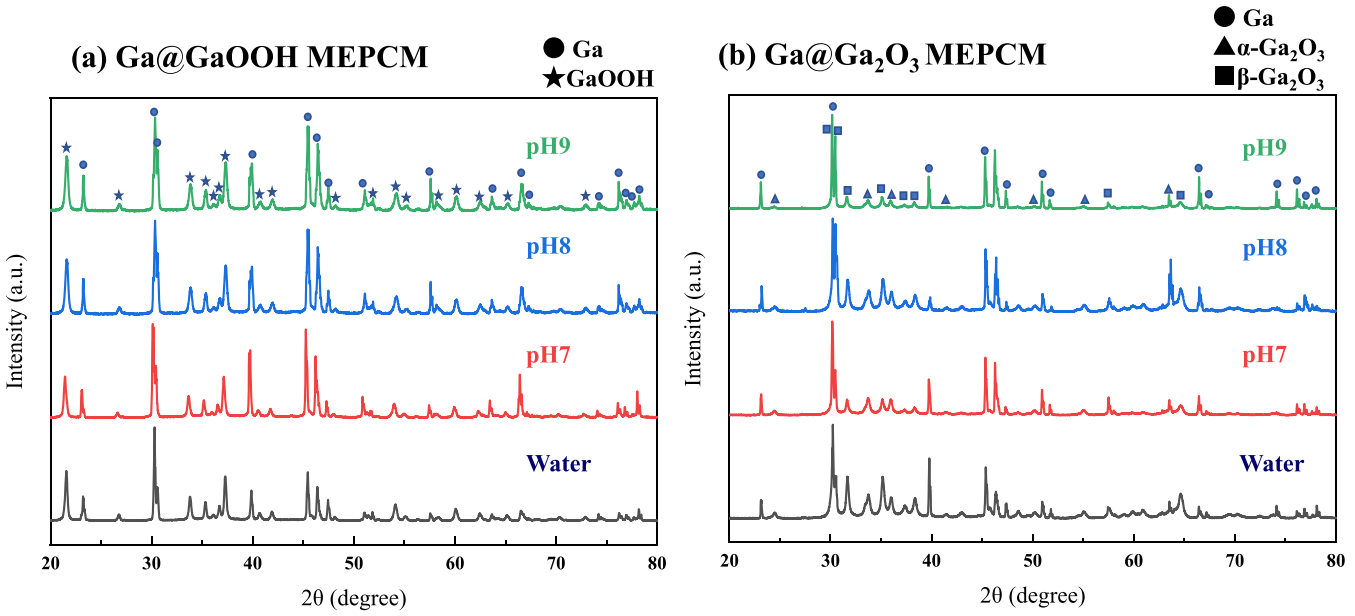

Figure 7. XRD patterns of (a) Ga@GaOOH MEPCM and (b) Ga@Ga_2O_3 MEPCM.

be reduced. All these advantages could assist in enhancing the durability of MEPCMs. The thickness and crystal size data suggest that pH 9 is the best fabrication condition for Ga@GaOOH MEPCM.

Figure 5 shows the SEM images of the MEPCM surface after calcination. Both water- and pH 9-treated MEPCM had a further oxidized shell after calcination, and the sample treated at pH 9 showed a better morphology with a lower breaking ratio and smaller crystal size, similar to that before calcination. Figure 6 shows cross-section SEM images and EDS elemental mapping results (Ga is marked in blue, and O is in red). EDS mapping (Figure 6b,e) showed a totally covered core−shell structure of Ga and oxidized Ga with no other elements, demonstrating the success of microencapsulation and showing that calcination had no harmful effect on the core−shell structure. Additionally, in the high-magnification images, the chemically treated shell (Figure 6c) has a structure consisting of precipitated rod-like crystals with structural voids. After calcination (Figure 6f), the shell is denser, and the thickness is slightly increased; this result reflects the shell-strengthening effect of calcination.

3.2. Shell Formation Mechanism of MEPCM. Figure 7 shows the XRD patterns of the MEPCMs after hydrothermal treatment and after calcination. The XRD results indicate that after hydrothermal treatment, the composition of the MEPCM was Ga (core) and GaOOH (shell). Wood et al.[25] calculated the distribution of mononuclear Ga at various temperatures and pH values; their investigation showed that $Ga(OH)^{4-}$ is predominant when the pH is higher than 5. Avivi et al.[26] investigated and reported two possible generation routes for GaOOH in solution; under alkaline conditions, GaOOH is produced via the decomposition of $Ga(OH)^{4-}$, with the co-generation of OH^- and H_2O. Therefore, in this experiment, we believe that GaOOH was generated at high temperatures and then precipitated on the surface of Ga droplets to form a shell. The shell thickness increases with the increase of pH until pH 9, high pH provides high concentration of OH^-, which can produce more $Ga(OH)^{4-}$, and increase the amount of generated GaOOH. The reaction during the hydrothermal treatment can be described as follows (when the pH is higher than 5)

$$Ga^{3+} + 4OH^- \rightarrow Ga(OH)_4^- \ (pH > 5) \quad (1)$$

$$Ga(OH)_4^- \rightarrow GaOOH(s) + OH^-(aq) + H_2O \ (95°C) \quad (2)$$

Figure 8 shows the TG curves of MEPCMs formed in distilled water (black curve) and pH 9 ammonia solution (blue curve),

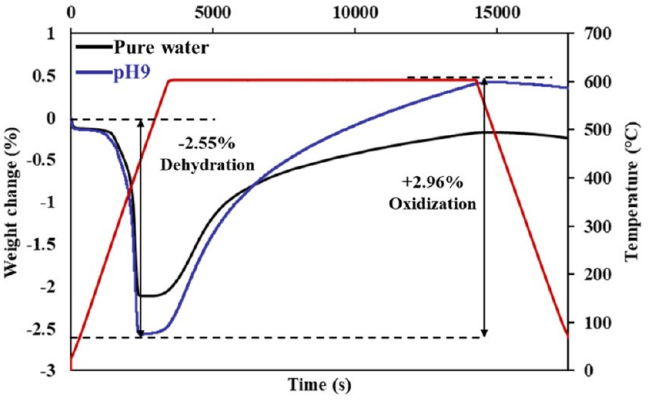

Figure 8. TG curves of Ga-MEPCM fabricated in pure water and pH 9 solution.

the red line shows the temperature history of the two samples. The samples were heated to 600 °C and maintained for 3 h under a 100 mL/min oxygen gas flow, with a heating speed of 10 K·min^{-1}. The weight and temperature change of the sample with time are shown in the figure. In the first stage (below 400 °C), the dehydration of GaOOH occurred; the sample was dehydrated and water vaporized as the temperature increased, and the GaOOH shell was completely converted into Ga_2O_3. The difference in the amount of weight loss (dehydration) implies that more GaOOH existed before calcination in the sample treated at pH 9; this result coincides with that of the shell thickness estimated from the cross-section. As the sample was further heated and oxidized, leakage and self-repairing

https://doi.org/10.1021/acsomega.2c02801
ACS Omega 2022, 7, 28313−28323

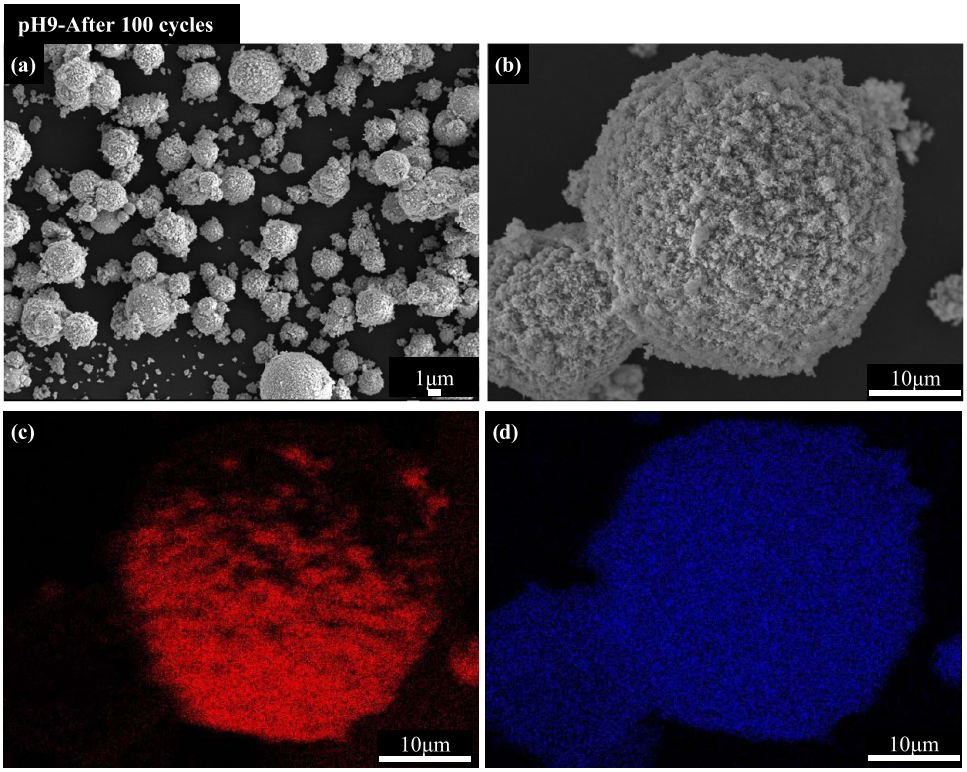

Figure 9. SEM images (a, b) and EDS mapping (c, d) of pH 9-treated Ga@Ga_2O_3 MEPCM after 100 cycles.

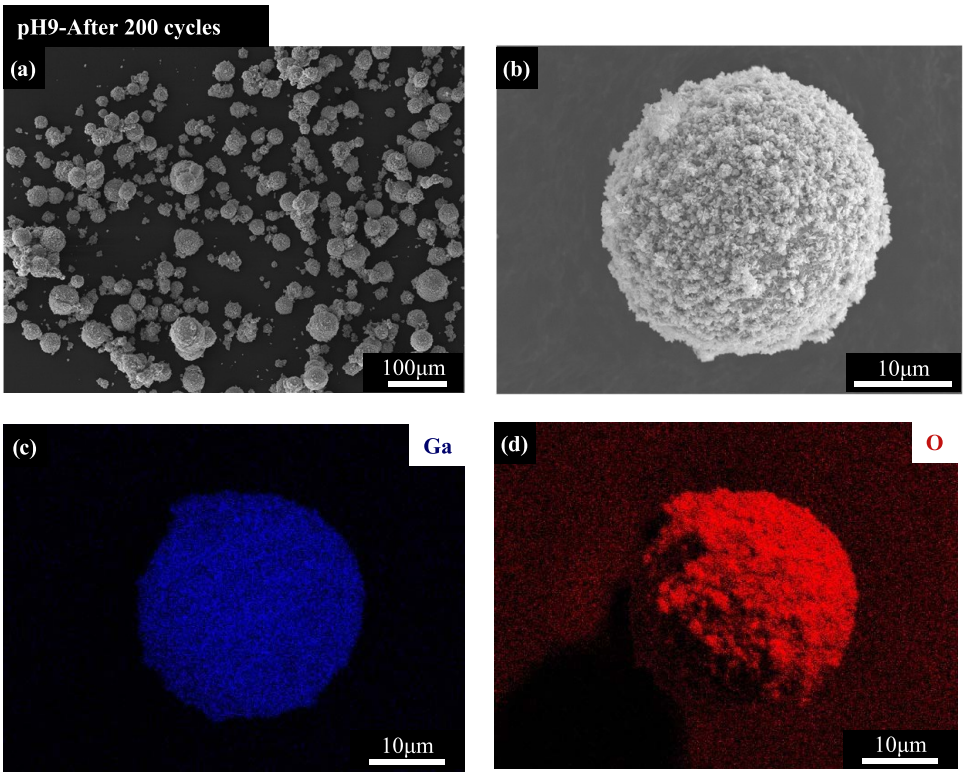

Figure 10. SEM images (a, b) and EDS mapping (c, d) of pH 9-treated Ga@Ga_2O_3 MEPCM after 200 cycles.

under an O_2 atmosphere occurred during heating and temperature maintenance, which has also been reported in previous studies.[16,27] During the high-temperature oxidation of metals, metal ions are generated in the shell, and diffusion of ions occurs along the concentration gradient. Therefore, the ions diffuse from the shell to the shell/gas interface and react with oxygen,[28] generating more Ga_2O_3 directly under an O_2 gas flow, which fills the structural voids and voids caused by dehydration; this explains the morphology change (denser and thicker shell) in Figure 6c,f. The structure of the MEPCM

https://doi.org/10.1021/acsomega.2c02801
ACS Omega 2022, 7, 28313−28323

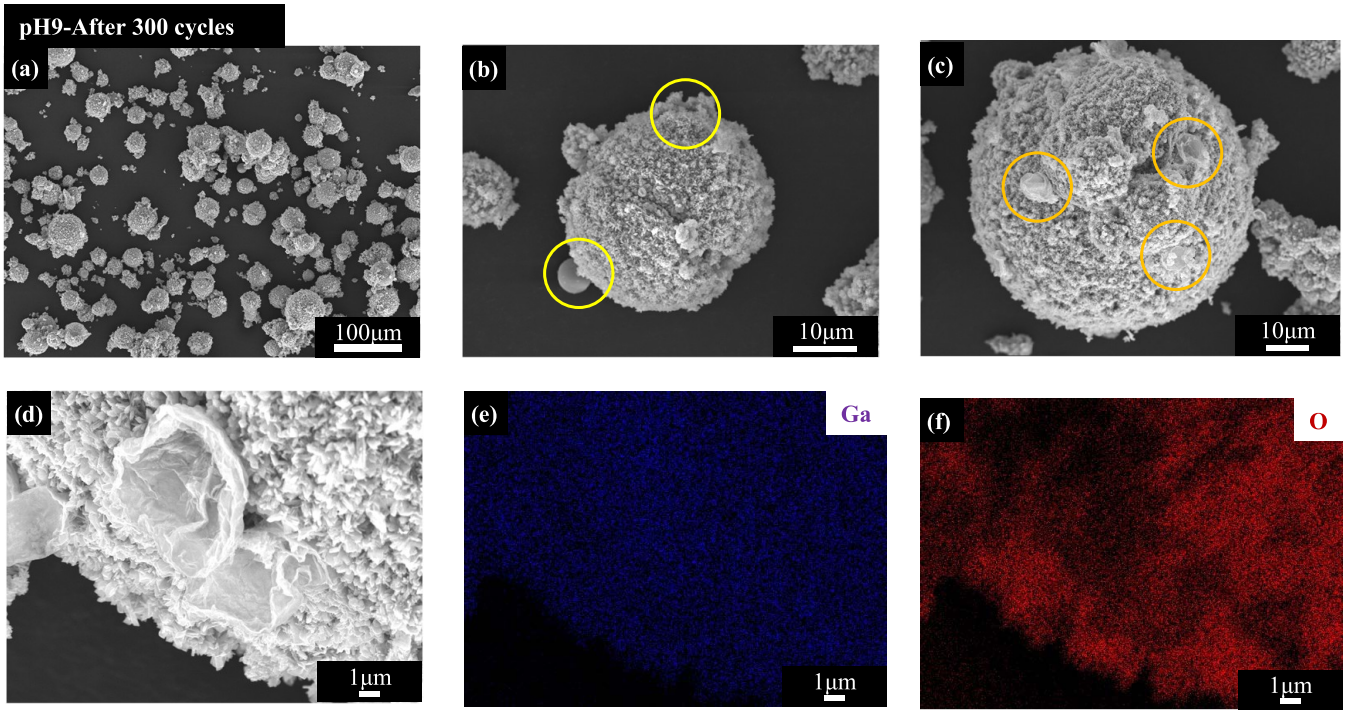

Figure 11. SEM images (a–d) and partial EDS mapping (e, f) of pH 9-treated Ga@Ga_2O_3 MEPCM after 300 cycles.

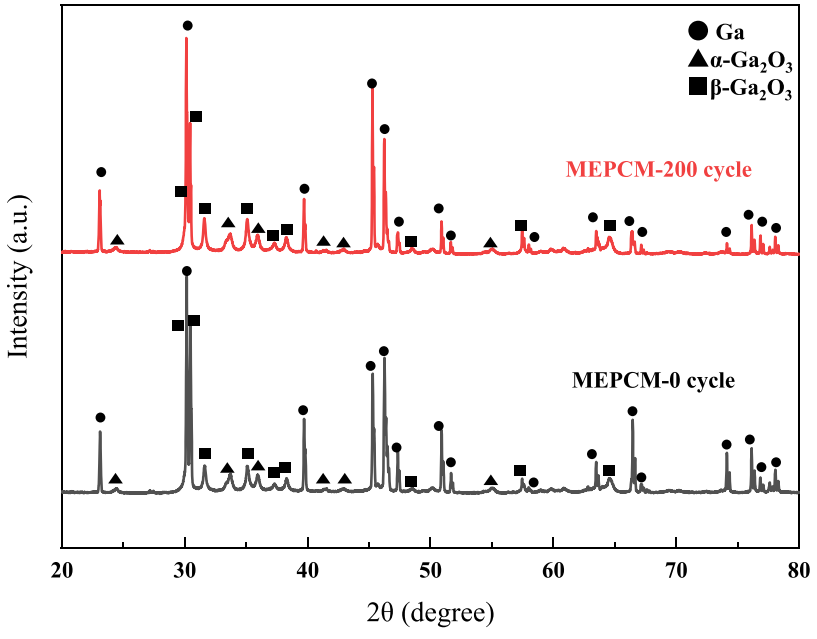

Figure 12. XRD patterns of Ga@Ga_2O_3 MEPCM before and after 200 thermal cycles.

transformed to that of Ga@Ga_2O_3 after calcination. Ga_2O_3 is the most stable compound among all the Ga oxides, and it has good chemical stability to resist corrosion and mechanical properties to resist expansion; with a Ga_2O_3 shell, the microcapsule could be more durable and stable. The reactions during calcination are as follows

$$2GaOOH(s) \rightarrow Ga_2O_3(s) + H_2O\ (\text{dehydration}) \quad (3)$$

$$Ga \rightarrow Ga^{3+} + 3e^{-}(\text{at the core/shell interface}) \quad (4)$$

$$\frac{1}{2}O_2 + 2e^{-} \rightarrow O^{2-}(\text{at the shell/gas interface}) \quad (5)$$

$$2Ga^{3+} + 3O^{2-} \rightarrow Ga_2O_3(\text{self} - \text{repair and Ga diffusion}) \quad (6)$$

After calcination, α-Ga_2O_3 and β-Ga_2O_3 were detected via XRD (in Figure 7), and no GaOOH could be observed. Wang et al.[29] investigated the GaOOH-Ga_2O_3 phase transition during calcination via XRD and Raman spectroscopy and suggested that the transition from α-Ga_2O_3 to β-Ga_2O_3 occurs from 590 to 630 °C without a change in the crystal size. After 3 h of calcination, most of the α-Ga_2O_3 phase transformed into

https://doi.org/10.1021/acsomega.2c02801
ACS Omega 2022, 7, 28313−28323

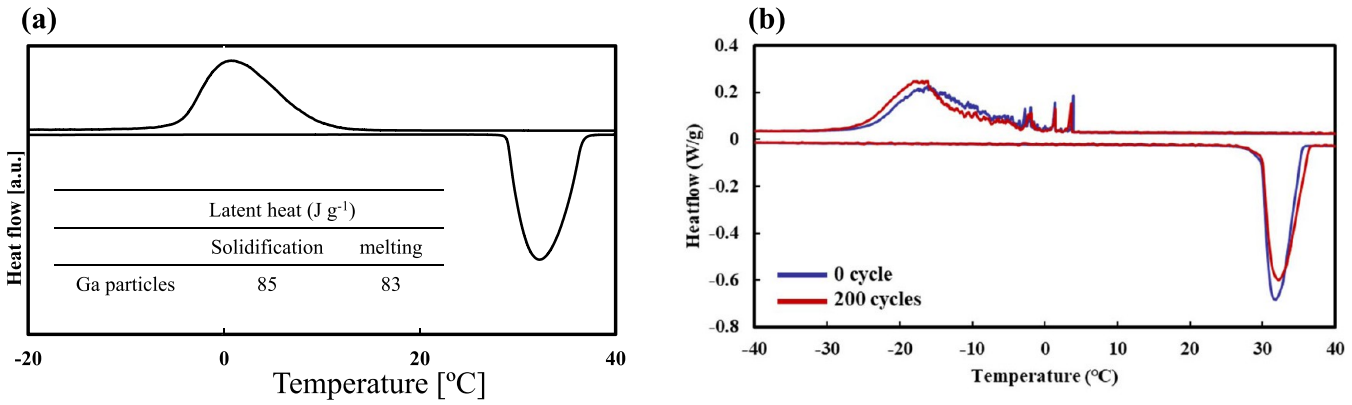

Figure 13. DSC curves of (a) pure Ga and (b) Ga@Ga_2O_3 MEPCM before and after durability test.

β-Ga_2O_3, which is the most stable phase of Ga_2O_3, with only a small amount of α phase remaining. XRD quantitative analysis also proved the predominance of the β phase in the MEPCM sample. A denser and more stable shell consisting of Ga_2O_3 was therefore formed after high-temperature calcination.

3.3. Durability of MEPCM. In practical applications, the LHS (latent heat storage) system is cyclically used many times, and the leakage of liquid metal PCM may also occur; this requires the PCM to have high durability. We investigated the durability of the as-prepared MEPCM using DSC, in which the MEPCM samples were heated to 50 °C and cooled to −50 °C rapidly (10 K·min^{-1}) to efficiently simulate practical utilization conditions in the lab. The surface morphology of the MEPCM samples after 100, 200, and 300 cycles was examined to determine their durability. Figures 9, 10, and 11 show the surface SEM images and EDS elemental mappings of MEPCM after 100, 200, and 300 cycles, respectively. After 100 and 200 cycles, all the MEPCM particles retain their shape, and no leakage from the Ga core is detected via SEM and EDS mapping. In some parts, the oxygen signal is weak because the uneven shell surface and spherical shape of the MEPCM lead to shielding during EDS analysis. We therefore, examined all the surfaces by rotating the sample at various angles to confirm this result. After 300 cycles, the MEPCM particles retained their shape, and no capsule collapse could be observed. However, we can clearly confirm the small amount of leakage of the Ga core in the MEPCM in many particles, in the yellow circles shown in Figure 11b,c, and using high-magnification SEM-EDS elemental mapping analysis shown in Figure 11d−f, we confirmed that the leaked part on the surface comprises exclusively Ga, without any O.

From the cross-section SEM images of the MEPCM, the shell consists of stacked Ga_2O_3 crystal rods, and there are many structural voids in the shell because of the rod shape of the crystals. These voids lead to mechanical defects, leaving defects in the shell. During thermal cycling, the metal core expands and shrinks several times, and the defect points in the shell will break first, and therefore, leakage will occur first at these points. This reflects the partial leakage of a small amount of the Ga core after 300 cycles, proving our estimation. This result also demonstrates the marked influence of the crystal size on durability, wherein smaller precursor crystals lead to structural voids and higher strength of the shell can be obtained, resulting in higher durability. In practical applications, the MEPCM can be embedded in polymer materials to eliminate the space between particles (for imparting heat transfer ability) or used as a PCM suspension; under these conditions, better durability can be expected, as there would be a binding force around the particle to further prevent particle collapse.[30−32] Figure 12 shows the XRD patterns of the MEPCM before and after 200 cycles, which proves the chemical stability of the MEPCM during cyclic tests. In summary, the MEPCM prevented the leakage of Ga and remained chemical stable for 200 cycles and maintained its particle shape for 300 cycles. Using the optimized hydrothermal treatment method, the durability of the MEPCM was significantly enhanced.

3.4. Heat Storage Performance of MEPCM. The heat storage capacity and melting and solidification characteristics before and after durability testing were investigated via DSC. Figure 13 shows the DSC curves of pure Ga and the MEPCM before thermal cycling and after 200 cycles. The latent heat of pure Ga is 85 J·g^{-1} for melting and 83 J·g^{-1} for solidification. The latent heat of the MEPCM is 60.6 J·g^{-1} (melting) and 59.08 J·g^{-1} (solidification) before testing and 57.84 J·g^{-1} (melting) and 57.50 J·g^{-1} (solidification) after 200 cycles. The MEPCM still has a high heat storage density after microencapsulation. The latent heat degradation is very low (~4.5%), which indicates that the MEPCM exhibits a stable heat storage capacity in long-term thermal cycles, suggesting the high durability of the MEPCM. The DSC curve also shows that the MEPCM has a larger amount of supercooling than the bulk pure Ga ingot, which demonstrates that microparticles always have a larger degree of supercooling than bulk specimens. Measures to reduce supercooling (such as the addition of nucleation agents or using a Ga alloy as a raw material) or the development of supercooling utilization (such as temperature-maintaining function for batteries and electronic parts under cold-weather conditions) for the MEPCM are needed in future research. The MEPCM retained the high rate of the heat storage capacity of the raw material after encapsulation and showed good stability in heat storage after many thermal cycles.

4. CONCLUSIONS

A microencapsulated Ga@Ga_2O_3 core−shell PCM was successfully fabricated. The optimal shell fabrication conditions and mechanism were investigated and discussed, and the microstructure and performance of the MEPCM were characterized. The conclusions can be summarized as follows:

(1) The most appropriate pH condition for hydrothermal treatment of Ga is pH 9. At pH 9, the sample showed the thickest shell and biggest amount of dehydration/

https://doi.org/10.1021/acsomega.2c02801
ACS Omega 2022, 7, 28313−28323

oxidation. After 3 h of treatment at pH 9 and 3 h of calcination at 600 °C, a stable and well-covered MEPCM was successfully fabricated. The experimental results also showed that pH has a strong influence on the crystal size of GaOOH; the MEPCM treated at pH 9 had a much smaller crystal size than the sample treated with distilled water.

(2) The durability of the MEPCM was significantly enhanced with the optimized fabrication method. The microcapsule sample showed no leakage after 200 cycles and maintained its particle shape until 300 cycles. The MEPCM also showed chemical stability during long-term durability testing.

(3) The MEPCM obtained a high heat storage capacity of 60.6 $J \cdot g^{-1}$ (melting) and 59.08 $J \cdot g^{-1}$ (solidification), corresponding to a high latent of 369.4 $J \cdot cm^{-3}$, which is ∼75% that of pure Ga. A high heat storage capacity with a low volume was achieved. Moreover, the MEPCM showed a very low latent heat degradation (∼4.5%) during the durability test, demonstrating the high reliability of the MEPCM.

■ ASSOCIATED CONTENT

Supporting Information

The Supporting Information is available free of charge at https://pubs.acs.org/doi/10.1021/acsomega.2c02801.

Particle size distribution of the MEPCM after hydrothermal treatment under each pH condition (PDF)

■ AUTHOR INFORMATION

Corresponding Author

Takahiro Nomura − *Faculty of Engineering, Hokkaido University, Sapporo, Hokkaido 060-8628, Japan;* orcid.org/0000-0003-3165-1386; Email: nms-tropy@eng.hokudai.ac.jp

Authors

Kaixin Dong − *Graduate School of Engineering, Hokkaido University, Sapporo, Hokkaido 060-8628, Japan*

Takahiro Kawaguchi − *Graduate School of Engineering, Hokkaido University, Sapporo, Hokkaido 060-8628, Japan*

Yuto Shimizu − *Graduate School of Engineering, Hokkaido University, Sapporo, Hokkaido 060-8628, Japan*

Hiroki Sakai − *Graduate School of Engineering, Hokkaido University, Sapporo, Hokkaido 060-8628, Japan*

Complete contact information is available at: https://pubs.acs.org/10.1021/acsomega.2c02801

Author Contributions

K.D.: writing − review and editing and investigation. T.K.: writing − review and editing. Y.S.: writing − review and editing. H.S.: writing − review and editing. T.N.: conceptualization, writing − review and editing and project administration.

Notes

The authors declare no competing financial interest.

■ ACKNOWLEDGMENTS

The scholarship support provided by the China Scholarship Council (CSC) during the doctoral course study of K.D. at Hokkaido University is acknowledged.

■ REFERENCES

(1) Babapoor, A.; Azizi, M.; Karimi, G. Thermal Management of a Li-Ion Battery Using Carbon Fiber-PCM Composites. *Appl. Therm. Eng.* **2015**, *82*, 281−290.

(2) He, Z.; Yan, Y.; Zhang, Z. Thermal Management and Temperature Uniformity Enhancement of Electronic Devices by Micro Heat Sinks: A Review. *Energy* **2021**, *216*, No. 119223.

(3) Li, Z.-w.; Lv, L.; Li, J. Combination of Heat Storage and Thermal Spreading for High Power Portable Electronics Cooling. *Int. J. Heat Mass Transfer* **2016**, *98*, 550−557.

(4) Safdari, M.; Ahmadi, R.; Sadeghzadeh, S. Numerical Investigation on PCM Encapsulation Shape Used in the Passive-Active Battery Thermal Management. *Energy* **2020**, *193*, No. 116840.

(5) Kandasamy, R.; Wang, X.-Q.; Mujumdar, A. S. Application of Phase Change Materials in Thermal Management of Electronics. *Appl. Therm. Eng.* **2007**, *27*, 2822−2832.

(6) Tomizawa, Y.; Sasaki, K.; Kuroda, A.; Takeda, R.; Kaito, Y. Experimental and Numerical Study on Phase Change Material (PCM) for Thermal Management of Mobile Devices. *Appl. Therm. Eng.* **2016**, *98*, 320−329.

(7) Ling, Z.; Zhang, Z.; Shi, G.; Fang, X.; Wang, L.; Gao, X.; Fang, Y.; Xu, T.; Wang, S.; Liu, X. Review on Thermal Management Systems Using Phase Change Materials for Electronic Components, Li-Ion Batteries and Photovoltaic Modules. *Renewable Sustainable Energy Rev.* **2014**, *31*, 427−438.

(8) Dong, K.; Sheng, N.; Zou, D.; Wang, C.; Shimono, K.; Akiyama, T.; Nomura, T. A High-Thermal-Conductivity, High-Durability Phase-Change Composite Using a Carbon Fibre Sheet as a Supporting Matrix. *Appl. Energy* **2020**, *264*, No. 114685.

(9) Zhang, Z.; Zhang, N.; Peng, J.; Fang, X.; Gao, X.; Fang, Y. Preparation and Thermal Energy Storage Properties of Paraffin/Expanded Graphite Composite Phase Change Material. *Appl. Energy* **2012**, *91*, 426−431.

(10) Zhang, P.; Ma, F.; Xiao, X. Thermal Energy Storage and Retrieval Characteristics of a Molten-Salt Latent Heat Thermal Energy Storage System. *Appl. Energy* **2016**, *173*, 255−271.

(11) Ge, H.; Li, H.; Mei, S.; Liu, J. Low Melting Point Liquid Metal as a New Class of Phase Change Material: An Emerging Frontier in Energy Area. *Renewable Sustainable Energy Rev.* **2013**, *21*, 331−346.

(12) Peng, H.; Guo, W.; Li, M.; Feng, S. Melting Behavior and Heat Transfer Performance of Gallium for Spacecraft Thermal Energy Storage Application. *Energy* **2021**, *228*, No. 120575.

(13) Liu, Z.; Chen, Z.; Yu, F. Preparation and Characterization of Microencapsulated Phase Change Materials Containing Inorganic Hydrated Salt with Silica Shell for Thermal Energy Storage. *Sol. Energy Mater. Sol. Cells* **2019**, *200*, No. 110004.

(14) Milián, Y. E.; Gutiérrez, A.; Grágeda, M.; Ushak, S. A Review on Encapsulation Techniques for Inorganic Phase Change Materials and the Influence on Their Thermophysical Properties. *Renewable Sustainable Energy Rev.* **2017**, *73*, 983−999.

(15) Onuki, R.; Ishii, K.; Fumoto, K.Preparation of Gallium Microcapsule Slurry and Evaluation of Heat Transport by Convection Experiment. *The 10th Latent Heat Engineering Symposium, Kobe, Japan, November 29th−30th*, 2021.

(16) Nomura, T.; Zhu, C.; Sheng, N.; Saito, G.; Akiyama, T. Microencapsulation of Metal-Based Phase Change Material for High-Temperature Thermal Energy Storage. *Sci. Rep.* **2015**, *5*, No. 9117.

(17) Sheng, N.; Zhu, C.; Saito, G.; Hiraki, T.; Haka, M.; Hasegawa, Y.; Sakai, H.; Akiyama, T.; Nomura, T. Development of a Microencapsulated Al−Si Phase Change Material with High-Temperature Thermal Stability and Durability over 3000 Cycles. *J. Mater. Chem. A* **2018**, *6*, 18143−18153.

(18) Sheng, N.; Zhu, C.; Sakai, H.; Hasegawa, Y.; Akiyama, T.; Nomura, T. Modified Preparation of Al2O3@Al-Si Microencapsulated Phase Change Material for High-Temperature Thermal Storage with High Durability over 3000 Cycles. *Sol. Energy Mater. Sol. Cells* **2019**, *200*, No. 109925.

(19) Bao, J.; Zou, D.; Zhu, S.; Ma, Q.; Wang, Y.; Hu, Y. A Medium-Temperature, Metal-Based, Microencapsulated Phase Change Ma-

terial with a Void for Thermal Expansion. *Chem. Eng. J.* **2021**, *415*, No. 128965.
(20) Kashiyama, K.; Kawaguchi, T.; Dong, K.; Sakai, H.; Sheng, N.; Kurniawan, A.; Nomura, T. Ga-based Microencapsulated Phase Change Material for Low-temperature Thermal Management Applications. *Energy Storage* **2020**, *2*, No. e177.
(21) Lin, Y.; Genzer, J.; Dickey, M. D. Attributes, Fabrication, and Applications of Gallium-Based Liquid Metal Particles. *Adv. Sci.* **2020**, *7*, No. 2000192.
(22) Krehula, S.; Ristić, M.; Kubuki, S.; Iida, Y.; Fabián, M.; Musić, S. The Formation and Microstructural Properties of Uniform α-GaOOH Particles and Their Calcination Products. *J. Alloys Compd.* **2015**, *620*, 217−227.
(23) Qian, H.-S.; Gunawan, P.; Zhang, Y.-X.; Lin, G.-F.; Zheng, J.-W.; Xu, R. Template-Free Synthesis of Highly Uniform α-GaOOH Spindles and Conversion to α-Ga_2O_3 and β-Ga_2O_3. *Cryst. Growth Des.* **2008**, *8*, 1282−1287.
(24) Zhao, Y.; Frost, R. L.; Yang, J.; Martens, W. N. Size and Morphology Control of Gallium Oxide Hydroxide GaO(OH), Nano- to Micro-Sized Particles by Soft-Chemistry Route without Surfactant. *J. Phys. Chem. C* **2008**, *112*, 3568−3579.
(25) Wood, S. A.; Samson, I. M. The Aqueous Geochemistry of Gallium, Germanium, Indium and Scandium. *Ore Geol. Rev.* **2006**, *28*, 57−102.
(26) Avivi, S.; Mastai, Y.; Hodes, G.; Gedanken, A. Sonochemical Hydrolysis of Ga^{3+} Ions: Synthesis of Scroll-like Cylindrical Nanoparticles of Gallium Oxide Hydroxide. *J. Am. Chem. Soc.* **1999**, *121*, 4196−4199.
(27) Nomura, T.; Yoolerd, J.; Sheng, N.; Sakai, H.; Hasegawa, Y.; Haga, M.; Akiyama, T. Al/Al2O3 Core/Shell Microencapsulated Phase Change Material for High-Temperature Applications. *Sol. Energy Mater. Sol. Cells* **2019**, *193*, 281−286.
(28) Taniguchi, S.; Kurokawa, K. *The Base and Application of High Temperature Oxidation—For the Development of Advanced Ultra High Temperature Material*; Uchida Rokakuho, 2006.
(29) Wang, X.; Xu, Q.; Fan, F.; Wang, X.; Li, M.; Feng, Z.; Li, C. Study of the Phase Transformation of Single Particles of Ga_2O_3 by UV-Raman Spectroscopy and High-Resolution TEM. *Chem. − Asian J.* **2013**, *8*, 2189−2195.
(30) Ma, Q.; Zou, D.; Wang, Y.; Lei, K. Preparation and Properties of Novel Ceramic Composites Based on Microencapsulated Phase Change Materials (MEPCMs) with High Thermal Stability. *Ceram. Int.* **2021**, *47*, 24240−24251.
(31) Jamekhorshid, A.; Sadrameli, S. M.; Barzin, R.; Farid, M. M. Composite of Wood-Plastic and Micro-Encapsulated Phase Change Material (MEPCM) Used for Thermal Energy Storage. *Appl. Therm. Eng.* **2017**, *112*, 82−88.
(32) Ho, C. J.; Chen, W.-C.; Yan, W.-M.; Amani, M. Cooling Performance of MEPCM Suspensions for Heat Dissipation Intensification in a Minichannel Heat Sink. *Int. J. Heat Mass Transfer* **2017**, *115*, 43−49.

https://doi.org/10.1021/acsomega.2c02801
ACS Omega 2022, 7, 28313−28323